J|A|C|S ARTICLES

Published on Web 05/07/2009

Conformational Changes of Channelrhodopsin-2

Ionela Radu,[†] Christian Bamann,[‡] Melanie Nack,[†] Georg Nagel,[§] Ernst Bamberg,[‡] and Joachim Heberle*,[†]

Bielefeld University, Biophysical Chemistry, 33615 Bielefeld, Max-Planck-Institute of Biophysics, Department of Biophysical Chemistry, 60438, Frankfurt/Main, and Würzburg University, Botany I, 97082 Würzburg, Germany

Received November 4, 2008; E-mail: joachim.heberle@uni-bielefeld.de

Abstract: Channelrhodopsin-2 (ChR2) is a member of the new class of light-gated ion channels which serve as phototaxis receptors in the green alga *Chlamydomonas reinhardtii*. The protein is employed in optogenetics where neural circuits are optically stimulated under high spatiotemporal control. Despite its rapidly growing use in physiological experiments, the reaction mechanism of ChR2 is poorly understood. Here, we applied vibrational spectroscopy to trace structural changes of ChR2 after light-excitation of the retinal chromophore. FT-IR difference spectra of the various photocycle intermediates revealed that stages of the photoreaction preceding (P_1 state) and succeeding (P_4) the conductive state of the channel (P_3) are associated with large conformational changes of the protein backbone as indicate by strong differences in the amide I bands. Critical hydrogen-bonding changes of protonated carboxylic amino acid side chains (D156, E90) were detected and discussed with regard to the functional mechanism. We used the C128T mutant where the lifetime of P_3 is prolonged and applied FT-IR and resonance Raman spectroscopy to study the conductive P_3 state of ChR2. Finally, a mechanistic model is proposed that links the observed structural changes of ChR2 to the changes in the channel's conductance.

Introduction

Two microbial-type rhodopsins were identified in the eyespot of the *Chlamydomonas reinhardtii* which are involved in phototaxis and photophobia of this unicellular green alga.[1,2] These rhodopsins define the new class of light-gated ion channels and, thus, have been named channelrhodopsin-1 (ChR1) and channelrhodopsin-2 (ChR2).[3] A model of the structure of ChR2 is depicted in Figure 1 where the retinal binding pocket is highlighted along with amino acids of particular relevance. Photocurrent measurements demonstrated that ChRs conduct both monovalent and divalent cations with protons showing the highest permeability.[4−6] Of particular note, ChR2 has been functionally expressed in mammalian neurons where it is able to drive neuronal depolarization by light (optogenetics).[7−9] The impact of ChR2 in neuroscience accentuates the need of deeper insights into the molecular mechanism of this key protein. Patch-clamp experiments provided first insights into the mechanism of ChR2[3] but these methods are devoid of structural sensitivity.

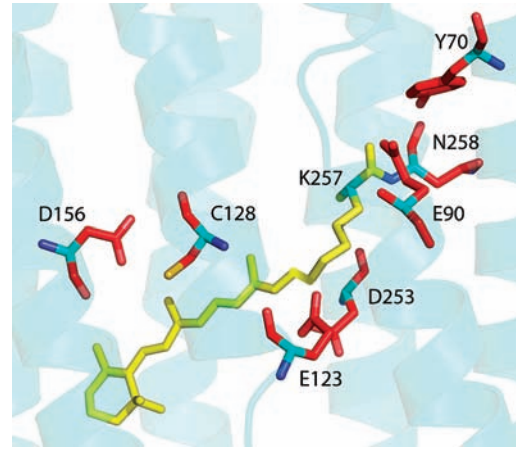

Figure 1. Model of the retinal binding pocket in ChR2 based on the crystal structure of sensory rhodopsin II from *Natronobacterium pharaonis* (Protein Data Bank access code 1gu8A.[55]) The transmembrane helices are shown as ribbons. The retinal chromophore (rendered in yellow) is bound to K257 (K216 in bR) via a protonated Schiff base linkage. The polar residues D156 (D115 in bR), C128 (T90), E123 (D85), D253 (D212), E90 (L62), Y70 (F42), and N258 (V217) are represented as sticks.

[†] Bielefeld University.
[‡] Max-Planck-Institute of Biophysics.
[§] Würzburg University.

(1) Foster, K. W.; Saranak, J.; Patel, N.; Zarilli, G.; Okabe, M.; Kline, T.; Nakanishi, K. *Nature* **1984**, *311* (5988), 756–759.
(2) Sineshchekov, O. A.; Jung, K. H.; Spudich, J. L. *Proc. Natl. Acad. Sci. U.S.A.* **2002**, *99* (13), 8689–8694.
(3) Nagel, G.; Szellas, T.; Kateriya, S.; Adeishvili, N.; Hegemann, P.; Bamberg, E. *Biochem. Soc. Trans.* **2005**, *33* (Pt 4), 863–866.
(4) Nagel, G.; Ollig, D.; Fuhrmann, M.; Kateriya, S.; Musti, A. M.; Bamberg, E.; Hegemann, P. *Science* **2002**, *296* (5577), 2395–2398.
(5) Nagel, G.; Szellas, T.; Huhn, W.; Kateriya, S.; Adeishvili, N.; Berthold, P.; Ollig, D.; Hegemann, P.; Bamberg, E. *Proc. Natl. Acad. Sci. U.S.A.* **2003**, *100* (24), 13940–13945.
(6) Berthold, P.; Tsunoda, S. P.; Ernst, O. P.; Mages, W.; Gradmann, D.; Hegemann, P. *Plant Cell* **2008**, *20* (6), 1665–1677.
(7) Boyden, E. S.; Zhang, F.; Bamberg, E.; Nagel, G.; Deisseroth, K. *Nat. Neurosci.* **2005**, *8* (9), 1263–1268.
(8) Zhang, F.; Wang, L. P.; Brauner, M.; Liewald, J. F.; Kay, K.; Watzke, N.; Wood, P. G.; Bamberg, E.; Nagel, G.; Gottschalk, A.; Deisseroth, K. *Nature* **2007**, *446* (7136), 633–639.
(9) Zhang, F.; Prigge, M.; Beyriere, F.; Tsunoda, S. P.; Mattis, J.; Yizhar, O.; Hegemann, P.; Deisseroth, K. *Nat. Neurosci.* **2008**, *11* (6), 631–633.

Two recent studies reported on the photocycle kinetics of ChR2 and identified photoproducts by time-resolved UV−vis spectroscopy.[10,11] The first photointermediate which could be detected after light excitation, denoted here P_1, is red-shifted down to 500 nm and has a risetime of 50 ns. P_1 decays with a time-constant of 4 μs to the next intermediate P_2. The absorption maximum of P_2 is blue-shifted ($\lambda_{max} = 390$ nm) and in analogy to the M intermediate of bacteriorhodopsin (bR) was concluded that the retinal has a deprotonated Schiff base. It follows a third intermediate P_3 with absorption maximum at 520 nm which rises with a time constant of $\tau = 150$ μs and decays with $\tau = 10$ ms. The P_3 kinetics is associated with opening and closing of the channel, respectively. The recovery of ground-state ChR2 ($\tau \approx 5$ s) involves the appearance of another intermediate P_4. It has the same absorption maximum as the ground state and its decay is associated with desensitization of the channel.

As UV−vis spectroscopy detects electronic changes only in the retinal chromophore, complementary techniques are required to monitor the conformational changes of the entire protein. FT-IR and resonance Raman spectroscopy have been very valuable vibrational techniques in resolving the functional changes of retinal proteins as exemplified by the seminal work on bR (see refs 12−15 for reviews). In the present work, we probed the structural changes of ChR2 by static and time-resolved vibrational spectroscopy. Our primary finding is that the channel activity is correlated with large conformational changes of the protein backbone as we detected large difference bands in the amide I region which manifest at the very early (in the P_1 state) and the very late stage (in the P_4 state) of the photoreaction. As the initial large backbone changes persist across the entire photoreaction, we infer that the gating process itself involves smaller structural changes - probably of just a few amino acids. Further molecular alterations, like proton transfer and hydrogen-bonding changes, assist the final step of the photoreaction. According to our data, the conformational changes of the protein are sensed by D156 on helix D (Figure 1) which is highly conserved in microbial rhodopsins. The corresponding residue in bR, D115, forms a hydrogen bond with T90 on helix C (C128 in ChR2),[16−18] and it is reasonable to assume that this hydrogen bond is maintained in ChR2. As this molecular interaction is considered to be of particular relevance to the photoreaction of bR, we studied the influence of the C128T mutation. In addition, the prolonged decay time of the (conductive) P_3 state observed in this mutant[19] allowed for the detailed investigation of the conductive state by vibrational spectroscopy. Finally, we discuss our results with respect to the reported electrical characteristics of ChR2 and present a model of the conformational changes accompanying channel activity.

Materials and Methods

Expression and Purification of ChR2. The cDNA of chop2 (Acc. No. AF461397) encoding for residues 1−315 plus a C-terminal 9xHis-tag sequence was cloned in the pPIC9K vector (Invitrogen) via its *Eco*RI and NotI sites. Point mutations at position C128 were inserted with the QuikChange kit (Stratagene) and confirmed by sequence analysis. The constructs were transformed after linearization in the *Pichia pastoris* strain SMD1163 (*his4*, *pep4*, *pbr*) (Invitrogen). Cell cultures and membrane preparations were performed as described[10,20] with the modification that membranes were homogenized in 20 mM Hepes/NaOH, pH 7.4, 100 mM NaCl and 1 mM PMSF. Membranes were solubilized in 1% [w/v] decyl maltoside (Glycon Biochemicals) and 2 M urea for 1 h at 4 °C. After centrifugation (100.000 g, 1 h), the supernatant was loaded on a Ni-NTA sepharose (GE Healthcare) and eluted with 500 mM imidazole. The protein samples were concentrated in Centrikon YM-10 concentrators (Millipore).

FT-IR Difference Spectroscopy. Ten microliters of a highly concentrated solution of wild-type ChR2 or C128T mutant dissolved in 0.2% decylmaltoside (stabilized by 5% sucrose, pH 7.4) was applied to a sandwich cell of two CaF_2 substrates which was inserted into a LN_2 cryostat (Oxford Instruments Limited). For ATR (attenuated total reflection) spectroscopy performed at 293 K, the solution was deposited to the surface of the diamond reflection element and sealed with a optically transparent lid.[21] We avoided to prepare rehydrated films in any of the IR measurements because we found that the protein is nonfunctional after drying. A light emitting diode (Luxeon Star, emission maximum at 462 and 30 nm fwhm, power density of 10 mW/cm^2) that closely matches the absorption spectrum of ChR2 was used for sample excitation. All infrared experiments were performed on an IFS 66v/S spectrometer (Bruker Optics, Ettlingen, Germany). The static FT-IR difference spectra represent an average of 20 000 scans at 293 K and of 5000 scans at 80 K. The spectral resolution was set to 4 cm^{-1} and a broadband interference filter (OCLI) limited the spectral range from 1900 to 850 cm^{-1}. Time-resolved infrared spectroscopy was performed in the rapid-scan mode with a time-resolution of 40 ms; 8000 repetitions of the light-induced experiment were averaged to improve the signal-to-noise ratio. For pulsed sample excitation, the output of an optical parametric oscillator (Opta, $\lambda = 462$ nm, 0.1 Hz repetition frequency, 3 mJ/cm^{-2} at sample position) driven by the frequency triplet output of a Nd:YAG laser (Quanta-Ray-Lab-Series, Spectra Physics, pulse duration 10 ns) was used.[22,23]

Resonance Raman Spectroscopy. Resonance Raman spectra were recorded on a LABRAM spectrometer (Jobin Yvon, Bensheim, Germany)[24] at the excitation wavelength of 647 nm line from a Krypton ion laser (Innova 90C, Coherent, Dieburg, Germany). A microscope objective (Olympus) focused the laser emission to a spot size of 20 μm with a power of 50 mW at the sample. The wavenumber increment per data point was 0.5 cm^{-1} and the spectral resolution was 2 cm^{-1}. One-hundred fifty microliters of detergent-solubilized C128T mutant (0.2 mM) was put into a rotating quartz cell spun at 1700 rpm. The protein was photoactivated by the 488 nm line from an argon ion laser (240 mW/cm^2,

(10) Bamann, C.; Kirsch, T.; Nagel, G.; Bamberg, E. *J. Mol. Biol.* **2008**, *375* (3), 686–694.
(11) Ernst, O. P.; Sanchez Murcia, P. A.; Daldrop, P.; Tsunoda, S. P.; Kateriya, S.; Hegemann, P. *J. Biol. Chem.* **2008**, *283* (3), 1637–1643.
(12) Mathies, R. A.; Lin, S. W.; Ames, J. B.; Pollard, W. T. *Annu. Rev. Biophys. Biophys. Chem.* **1991**, *20*, 491–518.
(13) Heberle, J. *Biochim. Biophys. Acta* **2000**, *1458* (1), 135–147.
(14) Kötting, C.; Gerwert, K. *ChemPhysChem* **2005**, *6* (5), 881–888.
(15) Vogel, R.; Siebert, F. *Curr. Opin. Chem. Biol.* **2000**, *4* (5), 518–523.
(16) Essen, L.; Siegert, R.; Lehmann, W. D.; Oesterhelt, D. *Proc. Natl. Acad. Sci. U.S.A.* **1998**, *95* (20), 11673–11678.
(17) Royant, A.; Edman, K.; Ursby, T.; PebayPeyroula, E.; Landau, E. M.; Neutze, R. *Nature* **2000**, *406*, 645–648.
(18) Luecke, H.; Schobert, B.; Richter, H. T.; Cartailler, J. P.; Lanyi, J. K. *J. Mol. Biol.* **1999**, *291* (4), 899–911.
(19) Berndt, A.; Yizhar, O.; Gunaydin, L. A.; Hegemann, P.; Deisseroth, K. *Nat. Neurosci.* **2009**, *12* (2), 229–234.
(20) Andre, N.; Cherouati, N.; Prual, C.; Steffan, T.; Zeder-Lutz, G.; Magnin, T.; Pattus, F.; Michel, H.; Wagner, R.; Reinhart, C. *Protein Sci.* **2006**, *15* (5), 1115–1126.
(21) Nyquist, R. M.; Ataka, K.; Heberle, J. *ChemBioChem* **2004**, *5* (4), 431–436.
(22) Majerus, T.; Kottke, T.; Laan, W.; Hellingwerf, K.; Heberle, J. *Chemphyschem* **2007**, *8* (12), 1787–1789.
(23) Pfeifer, A.; Majerus, T.; Zikihara, K.; Matsuoka, D.; Tokutomi, S.; Heberle, J.; Kottke, T. *Biophys. J.* **2009**, *96* (4), 1462–1470.
(24) Mironova, O. S.; Efremov, R. G.; Person, B.; Heberle, J.; Budyak, I. L.; Büldt, G.; Schlesinger, R. *FEBS Lett.* **2005**, *579* (14), 3147–3151.

Omnichrome, Melles Griot Laser Group, Carlsbad, Germany) resulting in the photostationary accumulation of the long-lived P_3 state.

UV−Vis Spectroscopy. Absorption difference spectra were recorded on an UV-2450 PC spectrometer (Shimadzu Corporation) with a sampling interval of 1 nm and a slit width of 2 nm. Eight micromolar of protein sample were solubilized in detergent and measured in a 0.5 cm quartz cuvette thermostatted to 293 K by a circulating water bath. The blue LED was used for sample excitation.

Time-resolved spectral changes of solubilized ChR2 (0.01 mM) in the seconds range were recorded on double beam spectrophotometer (U3000, Hitachi) with a light guide coupled to the quartz cuvette. The reaction was started by a laser flash from a broadband dye laser (RDP-1, Radiant Dye Laser Accesoires) pumped by a XeCl excimer laser (Lambda Physik). Energies for single flashes amounted to 0.25 to 0.5 mJ mm^{-2} for a Coumarin 2 ($\lambda = 456$ nm) solution.[10]

Results

Vibrational spectroscopy represents a particularly sensitive technique to study details of molecular reactions. To achieve sufficient selectivity in studies on proteins on the single vibrational level, either reaction-induced difference spectra between two states of the protein are recorded when using FT-IR spectroscopy or the resonance effect is exploited when Raman scattering is detected.[25] Thus, both techniques are complementary but resonance Raman spectroscopy selectively probes cofactor vibrations whereas FT-IR difference spectroscopy provides information on structural changes of the entire protein. To begin with, we applied light-induced FT-IR difference spectroscopy where positive bands correspond to the intermediate state and the negative bands to the dark state. Whereas P_1 and P_4 photointermediates are stabilized by an appropriate selection of the temperature,[10,11,26] the fast kinetics of the conducting state P_3 impedes its investigation by static infrared techniques. Therefore, we also performed experiments on the point mutant C128T (Figure 1) in which the lifetime of the conductive P_3 intermediate is delayed.[19]

FT-IR Analysis of the 80 K Intermediate (P_1) of ChR2. As well-known from other retinal proteins, also the P_1 intermediate of ChR2 can be trapped at 80 K,[26] where the thermal energy is not sufficient to overcome the transition barrier to the subsequent product. The difference spectrum at 80 K (Figure 2, top curve) exhibits vibrational changes in the fingerprint domain (1250−1150 cm^{-1}) that characterize the isomerization from the *all-trans* to the 13-*cis* configuration of the retinal chromophore. The intense positive band at 1191 cm^{-1} indicates the presence of 13-*cis* retinal with a protonated Schiff base, as it was established by the pioneering vibrational analyses on bR.[27,28] Bands of the C═C stretching vibration are expected in the region between 1500−1600 cm^{-1}. The strongest bands, originating from the symmetric stretching mode, cannot be unambigously localized in the infrared difference spectrum for both the ground state at 80 K and for P_1 state. Most probably, they are obscured by amide II vibrations (coupled C═N−H mode) that also contribute to this spectral region. Their identification will emerge from resonance Raman spectroscopy which selectively probes the chromophore in biological systems. Such experiments are currently underway.

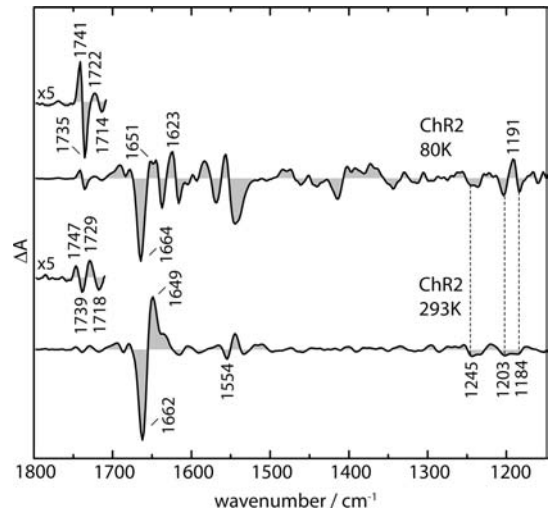

Figure 2. Light-induced infrared difference spectra of ChR2 at 80 K (top) and at 293 K (bottom) recorded under photostationary conditions. The spectra were scaled to the same intensities at 1245 cm^{-1}.

Remarkably and in stark contrast to all other retinal proteins, a strong negative band at 1664 cm^{-1} is manifested in the amide I range (C═O stretch of the peptide linkage). The occurrence of this band indicates large structural changes in the protein backbone.

Another feature of the transition to P_1 is the differential band feature at 1741(+)/1735(−) cm^{-1} appearing in the region specific to the C═O stretching vibration of carboxylic acid residues (Figure 2, expanded trace). A differential band feature at 1740(−)/ 1733(+) cm^{-1} was observed in bR which was assigned to a hydrogen-bonding change of protonated D115 on helix D.[29] However, the latter change is not only with opposite signs but also smaller in intensity than those observed in ChR2. Thus, we conclude that changes in the C═O stretching region of ChR2 are not solely attributable to D156. The differential band at 1741(+)/1735(−) cm^{-1} may include spectral features caused by proton transfer events with D156 as the proton donor. Another environmental change causes the differential band at 1722(+)/1714(−) cm^{-1} which shows a reduced intensity. Its location at lower frequencies is consistent with stronger hydrophilic exposure of the carboxylic residue which generates this band. Such a complex spectral feature indicating multiple rearrangements of hydrogen bonds at 80 K is expected since the protein undergoes large conformational changes which will inevitably perturb the pK_a of specific residues. The band pattern at 1741(+)/1735(−) cm^{-1} was also observed by Ritter et al.[26] In contrast, they were not able to resolve the red-shifted band features due to their lower signal-to-noise ratio.

FT-IR Analysis of the Late Intermediate P_4. Continuous blue-light illumination of ChR2 at 293 K generates a photostationary state of the long-lived intermediate P_4 with minor contributions from P_3.[10,11,26] The light-induced infrared difference spectrum recorded at this temperature (Figure 2, bottom curve) demonstrates that the large conformational change persists until the last photocycle intermediate as reflected by the strong bands in the amide I region. The intense amide I bands at 1662(−)/ 1649(+) cm^{-1} appears at frequencies typical for α-helices. We

(25) Siebert, F.; Hildebrandt, P. *Vibrational Spectroscopy in Life Science*; Wiley-VCH: Weinheim, 2007.
(26) Ritter, E.; Stehfest, K.; Berndt, A.; Hegemann, P.; Bartl, F. J. *J. Biol. Chem.* **2008**, *283* (50), 35033–35041.
(27) Gerwert, K.; Siebert, F. *EMBO J.* **1986**, *5* (4), 805–811.
(28) Smith, S. O.; Lugtenburg, J.; Mathies, R. A. *J. Membr. Biol.* **1985**, *85* (2), 95–109.
(29) Braiman, M. S.; Mogi, T.; Marti, T.; Stern, L. J.; Khorana, H. G.; Rothschild, K. J. *Biochemistry* **1988**, *27* (23), 8516–8520.

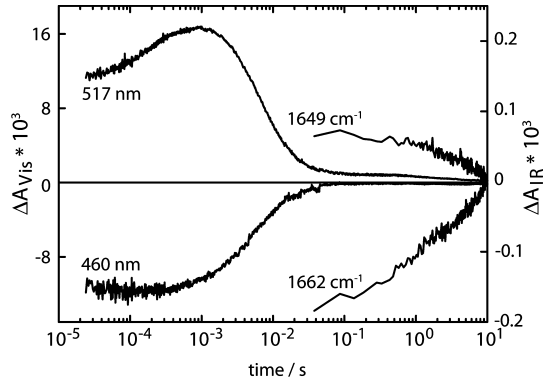

Figure 3. Room-temperature infrared kinetics monitored at 1662 and 1649 cm^{-1} as compared with the visible kinetics at 517 and 460 nm.

note that experiments on ChR2 reconstituted in lipids show the same large difference bands in the amide I region (data not shown). In the fingerprint domain, the spectrum of ChR2 exhibits hardly any contributions from the retinal chromophore as the intensities of the difference bands are negligible when compared to those at 80 K. The small negative band at 1554 cm^{-1} reflects the ethylenic mode of ground-state retinal as indicated by resonance Raman spectroscopy (see below). Thus, we conclude that ChR2 carries a retinal chromophore in the P_4 state with a similar geometry as the ground state albeit with a strong conformational distortion in the α-helical part of the surrounding opsin moiety.

The differential band at 1747(+)/1739(−) cm^{-1} is also observed in the light-induced difference spectrum of ChR2 at cryogenic temperature but at slightly lower frequencies (Figure 2, expanded traces). Since the band appears with a reduced intensity in the room temperature spectrum, we conclude that hydrogen-bonding changes of D156 that occur in the transition to the P_1 state, still manifest in the P_4 state. Besides D156, the pair of bands at 1729(+)/1718(−) cm^{-1} indicates that another carboxylic acid is subjected to changes in hydrogen bonding. This band was assigned to the C═O stretch of E90 on the basis of site-directed mutagenesis.[26]

Recovery of the Ground State. The kinetics of the photoreaction was recorded by rapid-scan FT-IR spectroscopy. Figure 3 shows the time-course of the absorbance changes after pulsed laser excitation of the amide I bands at 1662 and at 1649 cm^{-1}, respectively. It is obvious that the structural changes as reflected by the amide I bands, decay much slower than the kinetics monitored in the visible (traces measured at 460 and 517 nm). This result provides firm evidence that closing of the channel which coincides with the decay of the P^{520} intermediate, proceeds at a rate of almost 3 orders of magnitude faster than the large conformational changes of the protein backbone! Close inspection of the time trace at 517 nm reveals that a weak absorption change is still discernible in the ms-s time range. The decay of the latter correlates with that of the amide I bands. The very slow kinetics were interpreted to be due to the desensitization of the channel.[5] Thus, our data reveal that the closed desensitized state rather than the conducting state is associated with large distortions of the protein backbone.

P_3 State in the C128T Mutant. The exchange of C128 to T leads to a 1.000 times slower decay of the P_3 intermediate.[19] Thus, continuous illumination of the C128T mutant at 293 K creates a photostationary state with a higher content of P_3 than in wild-type ChR2. The UV−vis difference spectrum of the C128T mutant (solid trace in Figure 4) reflects a 5 nm red-shifted of the ground-

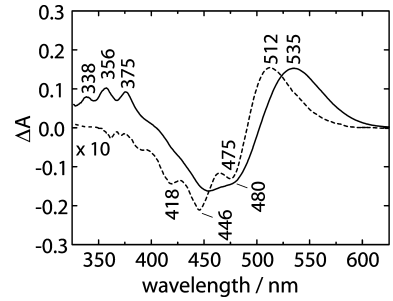

Figure 4. UV−vis difference spectra of the C128T mutant (solid line) and of wild-type ChR2 (dashed line) recorded under photostationary conditions.

state absorption along with a significant loss of vibronic fine structure as compared to the wild type (dashed trace). This result agrees with the observed blue-shift in ground-state absorption in a variant of bR where the corresponding threonine residue was replaced by Cys (T90C).[30] The positive absorption in the UV−vis difference spectrum is red-shifted by 23 nm in the C128T mutant (from 512 nm in wild-type ChR2 to 535 nm in the mutant) indicating the presence of the P_3 state. In contrast to the wild type, however, the mutant spectrum also includes difference bands in the UV region with maxima at 338, 356, and 375 nm. These are characteristic to retinal with deprotonated Schiff base and indicate the presence of the P_2 state.

The photostationary state of the C128T mutant was examined by FT-IR difference spectroscopy (Figure 5, top spectrum). It is evident that the prominent amide I difference bands that were observed in wild-type ChR2 (bottom spectrum of Figure 2,) also appear in the C128T spectrum indicating that the predominant P_3 state of the photostationary state also exhibits a strongly altered backbone conformation. Yet, close inspection of the difference spectrum reveals a positive band at 1625 cm^{-1} that is not apparent in the wild-type spectrum. The frequency is typical for β-sheets and indicates additional structural alterations different from the P_4 state discussed above. Interestingly, a

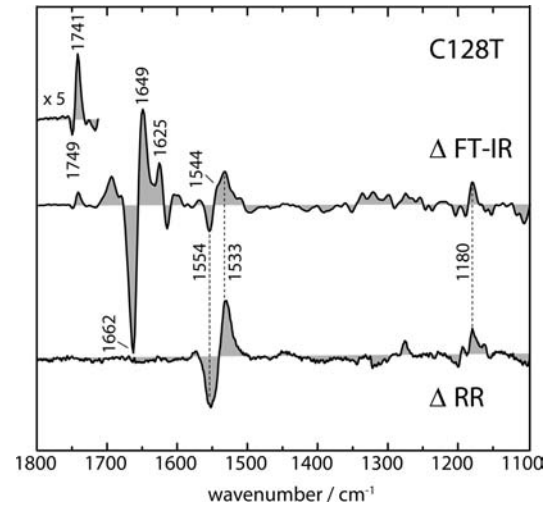

Figure 5. Vibrational spectroscopy on the C128T mutant of ChR2. Top spectrum: Light-induced FT-IR difference spectrum (ΔFT-IR) of the C128T mutant recorded under photostationary conditions at 293 K. Bottom spectrum: Resonance Raman difference spectrum (ΔRR) between the ground state of the C128T mutant and the accumulated photostationary state. The subtraction factor between the two RR spectra was chosen to mimic the FT-IR differences.

similar band is also present in the 80 K spectra of both wild-type ChR2 (Figure 2, top curve) and of the C128T mutant (data not shown).

The light-induced FT-IR difference spectrum (top spectrum in Figure 5) is compared to the resonance Raman difference spectrum (bottom spectrum). Preresonant conditions ($\lambda_{ex} = 647$ nm) were chosen to avoid the accumulation of intermediate states during the recording of the ground-state spectrum. Under continuous illumination of the C128T mutant with additional blue light, the P_3 intermediate is predominantly probed. The ground state contributes to the RR spectrum by $\sim 40\%$ under the applied photostationary conditions. Contaminations from vibrations of the P_2 state are absent because the electronic transitions are located in the UV range (see Figure 4) and are, therefore, not significantly enhanced by the Raman probe at 647 nm. Because the resonance effect selects for the retinal vibrations, the assignment of the retinal modes in the FT-IR difference spectrum is feasible. The strongest differences in the resonance Raman difference spectrum occur at 1554(−)/1533(+) cm^{-1} [31] and are assigned to the C=C symmetric stretching vibration of retinal in the ground-state and the P_3 state, respectively. The frequencies tally with the visible absorption maximum of the ground and the P_3 state as expected by the well-established correlation of the ethylenic stretch of retinal and the electronic transition.[32] In the FT-IR difference spectrum, a shoulder is present at 1544 cm^{-1} which might originate from changes in the amide II mode that are expected from the occurrence of strong bands in the amide I region. The fingerprint region exhibits a positive band at 1180 cm^{-1} which is indicative for 13-*cis* retinal with protonated Schiff base. The assignment of the retinal Schiff base vibration was not possible due to the limited signal-to-noise ratio.

As the P_3 state represents the conductive state of ChR2, it is of particular interest to study the changes in the C=O region of the carboxylic amino acid side chains as ion flow may induce changes in protonation state and/or in hydrogen-bonding of aspartic or glutamic acids. The negative band at 1739 cm^{-1} assigned to protonated D156 in the ground-state ChR2 (Figure 2, bottom) shifts to 1749 cm^{-1} in the mutant (Figure 5, expanded spectrum). The upshift by about 10 cm^{-1} is caused by the weakening of the hydrogen-bonding of the carbonyl oxygen induced by the exchange from the cysteine residue of the wild-type to the threonine of the mutant. The positive band at 1741 cm^{-1} is pronounced in this spectral domain and may indicate the protonation of an Asp/Glu residue. Another important observation in the C128T spectrum is the disappearance of the E90 bands of the wild type at 1729(+)/1718(−) cm^{-1}. On the basis of the structural model (Figure 1), the mutual distance of C128 and E90 is too large for immediate interaction. The experiments rather imply that the hydrogen bonding changes of E90 exclusively occur during the lifetime of the P_4 intermediate and the lower accumulation of P_4 in the C128T mutant causes the disappearance of the E90 bands. Thus, the hydrogen-bonding changes are related to the presence of the P_4 state.

Discussion

In searching for structural details which determine the specific function of ChR2, we performed a vibrational spectroscopic investigation of the wild-type protein and the C128T mutant. Most prominently, the recorded IR difference spectra are characterized by intense amide I bands which demonstrate that the protein undergoes large conformational changes along the photoreaction. Such a large extent of conformational changes is not experienced by any microbial rhodopsin so far investigated.[33−42]

To address the sequence of such molecular events, information on the temporal occurrence of the observed structural changes is essential. Infrared data taken at cryogenic temperatures (Figure 2, top spectrum) indicate that ChR2 undergoes large backbone alterations as soon as in the very early stage of the photoreaction. We suggest that the large structural alterations of ChR2 observed at 80 K occur on a subnanosecond timescale. This rationale is derived from pioneering experiments on bR[43] that relate the K state with ps rise and μs decay times at room temperature[12] to the K state that is trapped at cryogenic temperature where the thermal energy is insufficient for the transition to the subsequent photocycle intermediate (L). Despite the close similarity in the protein part, time-resolved IR spectra showed the retinal configuration more relaxed in the room temperature K intermediate.[44,45] Because the P_1 intermediate obtained at cryogenic temperatures is distinct from the conductive P_3 state, our data indicate that the backbone alterations observed in the former are not associated with the ion conductance but rather define the formation of the pore. The large structural changes persist to the final photointermediate P_4 as indicated by the intense amide I bands in the room temperature spectrum of ChR2 (Figure 2, bottom spectrum). The frequency of the amide I difference bands suggest that they are due to backbone changes in the α-helical part of the protein. Comparing the time-course of the amide I bands to the kinetics of P_3 decay (Figure 3), we found that the former are much slower. The observed structural changes correlate with the closed inactivated (or desensitized) state which succeeds channel closure.

(30) Flitsch, S. L.; Khorana, H. G. *Biochemistry* **1989**, *28* (19), 7800–7805.
(31) Smith, S. O.; Braiman, M. S.; Myers, A. B.; Pardoen, J. A.; Courtin, J. M. L.; Winkel, C.; Lugtenburg, J.; Mathies, R. A. *J. Am. Chem. Soc.* **1987**, *109* (10), 3108–3125.
(32) Aton, B.; Doukas, A. G.; Callender, R. H.; Becher, B.; Ebrey, T. G. *Biochemistry* **1977**, *16* (13), 2995–2999.
(33) Zscherp, C.; Heberle, J. *J. Phys. Chem. B* **1997**, *101* (49), 10542–10547.
(34) Rothschild, K. J.; Bousche, O.; Braiman, M. S.; Hasselbacher, C. A.; Spudich, J. L. *Biochemistry* **1988**, *27* (7), 2420–2424.
(35) Bousche, O.; Spudich, E. N.; Spudich, J. L.; Rothschild, K. J. *Biochemistry* **1991**, *30* (22), 5395–5400.
(36) Hein, M.; Wegener, A. A.; Engelhard, M.; Siebert, F. *Biophys. J.* **2003**, *84* (2), 1208–1217.
(37) Friedrich, T.; Geibel, S.; Kalmbach, R.; Chizhov, I.; Ataka, K.; Heberle, J.; Engelhard, M.; Bamberg, E. *J. Mol. Biol.* **2002**, *321* (5), 821–838.
(38) Furutani, Y.; Kawanabe, A.; Jung, K. H.; Kandori, H. *Biochemistry* **2005**, *44* (37), 12287–12296.
(39) Bergo, V.; Spudich, E. N.; Spudich, J. L.; Rothschild, K. J. *Photochem. Photobiol.* **2002**, *76* (3), 341–349.
(40) Hessling, B.; Herbst, J.; Rammelsberg, R.; Gerwert, K. *Biophys. J.* **1997**, *73* (4), 2071–2080.
(41) Moukhametzianov, R.; Klare, J. P.; Efremov, R.; Baeken, C.; Goppner, A.; Labahn, J.; Engelhard, M.; Buldt, G.; Gordeliy, V. I. *Nature* **2006**, *440* (7080), 115–119.
(42) Gmelin, W.; Zeth, K.; Efremov, R.; Heberle, J.; Tittor, J.; Oesterhelt, D. *Photochem. Photobiol.* **2007**, *83* (2), 369–377.
(43) Lozier, R. H.; Bogomolni, R. A.; Stoeckenius, W. *Biophys. J.* **1975**, *15* (9), 955–962.
(44) Weidlich, O.; Siebert, F. *Appl. Spectrosc.* **1993**, *47* (9), 1394–1400.
(45) Sasaki, J.; Yuzawa, T.; Kandori, H.; Maeda, A.; Hamaguchi, H. *Biophys. J.* **1995**, *68* (5), 2073–2080.

To get particular insights into the molecular events that accompany channel opening, we performed spectroscopic experiments on the C128T mutant which exhibits retarded decay kinetics of the P_3 intermediate. The vibrational (FT-IR and resonance Raman) spectra recorded at room temperature (Figure 5) clearly indicate the accumulation of a red-shifted intermediate with 13-*cis* retinal and protonated Schiff base which characterizes the retinal configuration in the P_3 state. In addition, the FT-IR difference spectrum of the C128T mutant shows a positive amide I band at 1625 cm^{-1} with the frequency typical for β-sheets. A similar band is also seen in the 80 K spectra both of ChR2 and C128T (data not shown). These observations point to structural changes different from those discussed above, which accompany pore formation. These structural distortions relax prior to P_4 formation because the corresponding bands do not show up in the P_4 spectrum of ChR2. Their assignment to β-sheet alterations infers that such segments undergo movements during channel gating. It is interesting to note here that the structural analysis of visual rhodopsin[46] revealed an intradiscal loop which forms a plug of β-sheets hindering rapid hydrolysis of the retinal Schiff base linkage.[47] The presence of such a plug in ChR2 would mark a common structural feature among rhodopsins.

The sequence of structural events after photoactivation elucidated by our FT-IR experiments are correlated to channel opening and closure which are determined by electrometric methods[10] and presented as a sketch in Figure 6. In the initial transition from ground-state ChR2 to the P_1 intermediate, the apoprotein undergoes large conformational changes affecting not only the helical part of the protein backbone but also elements of β-sheet structure. These fast and large conformational changes are interpreted in terms of the formation of the pore. Because this early reaction intermediate is not conductive, we conclude that the large conformational change does not yet generate a continuous pore across the membrane. The transition to the next intermediate state P_2 is accompanied by the deprotonation of the retinal Schiff base. Electrometric experiments on wild-type ChR2 suggested that the channel is still closed in P_2.[10] At the moment, we have no further structural information available on this reaction intermediate. The occurrence of the subsequent P_3 intermediate is associated with opening of the gate of the channel.[10] This central gating process succeeds the large structural changes involved in pore formation and may comprise only a few amino acids. The reversal of the large conformational changes succeeds channel closure and is associated with the desensitized state P_4. Interestingly, this process is very slow, completing in the range of seconds (Figure 3), as compared to the onset which occurs in the nanosecond time range. Such slow recovery kinetics of the initial conformation of the protein seems to be a notable trait of sensory rhodopsins and was suggested to be important to efficient signal transduction.[36,48,49]

The present infrared data also demonstrate that two amino acids are highly sensitive to the structural alterations which take place upon photoactivation of ChR2. Protonated D156 (on putative helix D) forms an interhelical hydrogen bond with C128 (on putative helix C). This hydrogen-bond is analogous to D115 of bR albeit with T90 as the partner in H-bonding.[50] The H-bonding environment of D156 is altered immediately after light-activation and accompanies pore formation, is also influenced by gating of the channel and finally relaxes during recovery of the initial state. Electrostatic calculations suggested that D115 of bR represents the sensor of the transmembrane potential.[51] Since the membrane potential modulates the activity of ChR2,[3,52] the elucidation of the functional role of the corresponding D156 bears great relevance. We infer that D156 plays a crucial role in the mechanism of ion channeling of ChR2. The other amino acid subjected to environmental changes during the photoreaction of ChR2 is E90 as proposed by Ritter et al.[26] According to the structural model (Figure 1), this residue locates on helix B (where also other five glutamates can be found) close to the Schiff base. It is still unclear which amino acid participates in the hydrogen bond with protonated E90 but Y70 and N258 may be good candidates. Our data suggest that the hydrogen bond is modified during the final decay of the (desensitized) P_4 state to the ground state of ChR2.

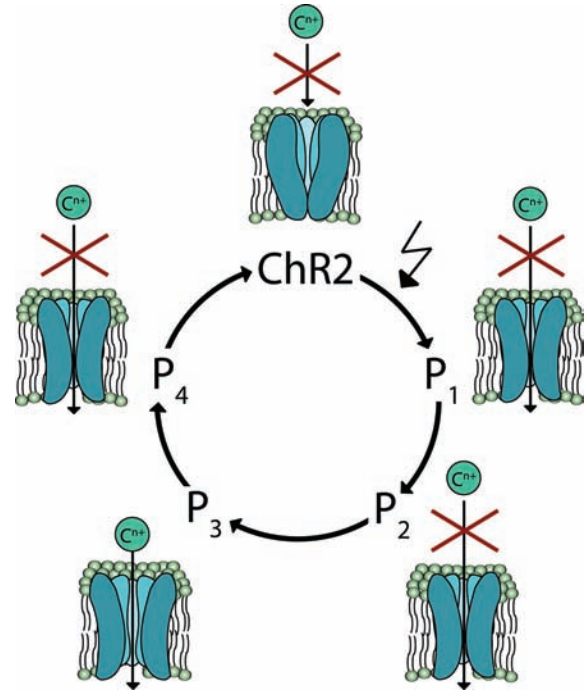

Figure 6. Sequence of conformational changes of ChR2 as deduced from the present infrared spectroscopic data. The structural events are correlated to channelling activity as measured by electrometric methods.[10] Channelrhodopsin-2 (ChR2) is activated by photon absorption of all-*trans* retinal. The *trans*−*cis* isomerization leads to alterations in the protein backbone conformation. However, this P_1 state is nonconductive (crossed arrow). The subsequent P_2 intermediate is characterized by a deprotonated retinal Schiff base but we infer that the backbone conformation is not significantly changed as compared to the previous P_1 state. P_2 decays to the conducting state P_3 where movement of a few residues may enable the flow of cations. Closing of the channel coincides with the formation of the P_4 intermediate together with the reversal of the retinal configuration from *cis* to *trans*. The large conformational changes of the protein backbone relax during the final transition from the desensitized P_4 state to the initial ground-state ChR2.

(46) Palczewski, K.; Kumasaka, T.; Hori, T.; Behnke, C. A.; Motoshima, H.; Fox, B. A.; LeTrong, I.; Teller, D. C.; Okada, T.; Stenkamp, R. E.; Yamamoto, M.; Miyano, M. *Science* **2000**, *289*, 739–745.
(47) Janz, J. M.; Fay, J. F.; Farrens, D. L. *J. Biol. Chem.* **2003**, *278* (19), 16982–16991.
(48) Bogomolni, R. A.; Spudich, J. L. *Biophys. J.* **1987**, *52* (6), 1071–1075.
(49) Chizhov, I.; Schmies, G.; Seidel, R.; Sydor, J. R.; Luttenberg, B.; Engelhard, M. *Biophys. J.* **1998**, *75* (2), 999–1009.
(50) Garczarek, F.; Gerwert, K. *J. Am. Chem. Soc.* **2006**, *128* (1), 28–29.
(51) Bombarda, E.; Becker, T.; Ullmann, G. M. *J. Am. Chem. Soc.* **2006**, *128* (37), 12129–12139.
(52) Hegemann, P. *Annu. Rev. Plant Biol.* **2008**, *59*, 167–189.

The present vibrational spectroscopic study traces a promising direction toward detailed investigations necessary to understand the structure and the molecular mechanism of this intriguing protein. The work sets the basis for vibrational studies that address the dependence of the channel conductance on the membrane potential. Here, the newly developed surface-enhanced FT-IR difference spectroscopy[53,54] will provide molecular resolution to the gating mechanism. From a physiological perspective, resolving those processes that bridge the two functions of ChR2 as ion channel and as phototaxis receptor will be of prime interest to the molecular understanding of signal transduction by ChR2.

Acknowledgment. This work was supported by grants from the Deutsche Forschungsgemeinschaft (SFB 613, A8) to J.H., (SFB 487, A12) to G.N., (SFB 472 and 807) to E.B., and by the Cluster of Excellence Frankfurt (Macromolecular Complexes). We thank Anja Becker for excellent technical assistance.

JA8084274

(53) Jiang, X.; Zaitseva, E.; Schmidt, M.; Siebert, F.; Engelhard, M.; Schlesinger, R.; Ataka, K.; Vogel, R.; Heberle, J. *Proc. Natl. Acad. Sci. U.S.A.* **2008**, *105* (34), 12113–12117.

(54) Ataka, K.; Heberle, J. *Anal. Bioanal. Chem.* **2007**, *388* (1), 47–54.

(55) Edman, K.; Royant, A.; Nollert, P.; Maxwell, C. A.; Pebay-Peyroula, E.; Navarro, J.; Neutze, R.; Landau, E. M. *Structure (Camb.)* **2002**, *10* (4), 473–482.